Journal of Systems Engineering and Electronics
Vol. 32, No. 3, June 2021, pp.607 – 618

Cluster segmentation algorithm based on the Vicsek with static summoning points

MA Yan[1,2], MAO Zhaoyong[1,*], QIN Jian[2], MENG Xiangyao[2], XIAO Yujie[2], CHEN Jianhua[2], and FENG Wei[2]

1. Key Laboratory of Unmanned Underwater Vehicle, Ministry of Industry and Information Technology, School of Marine Science and Technology, Northwestern Polytechnical University, Xi'an 710072, China; 2. Naval Research Academy, Beijing 100161, China

Abstract: Because of the low convergence efficiency of the typical Vicsek model, a Vicsek with static summoning points (VSSP) algorithm based on the Vicsek model considering static summoning points is proposed. Firstly, the mathematical model of the individual movement total cost on each summoning point is established. Then the individual classification rule is designed according to the initial state of the cluster to obtain the subclusters guided by each summoning point. Finally, the summoning factor is introduced to modify the course angle updating formula of the Vicsek model. To verify the effectiveness of the proposed algorithm and study the effect of the cluster summoning factor on the convergence rate, three groups of simulation experiments under different summoning factors are designed in this paper. To verify the superiority of the VSSP algorithm, the performance of the VSSP algorithm is compared with the classic algorithm by designing the algorithm performance comparison verification experiment. The results show that the algorithm proposed in this paper has good convergence and course angle consistency. The summoning factor is the sensitive factor of cluster convergence. This algorithm can provide a reference for efficient cluster segmentation movement.

Keywords: static summoning point, Vicsek model, summoning factor, cluster system.

DOI: 10.23919/JSEE.2021.000052

1. Introduction

Cluster system is ubiquitous in nature and human life, which has important practical significance for the study of cluster movement. The application research of cluster system has been widely carried out in many fields, such as the control and evolution of aviation clusters [1], leader-missile follower-missile cluster distributed guidance [2], time-varying formation tracking control [3], unmanned aerial combat system [4–9] and so on. In recent years, with the development of underwater unmanned systems, the intelligent technology of underwater clusters has been highly valued, which is of great significance to the research on the movement model of underwater cluster systems.

The research on cluster systems is mainly realized by establishing corresponding models. Typical cluster models include the Vicsek model, the Boid model, the three-circle model, the leader-follower model, and so on. However, these classic models have their shortcomings, so many scholars have improved them to enhance the performance of models. Given the slow convergence speed and low consistency of the Vicsek model, Gao et al. [10] proposed a new method to improve the convergence efficiency of the Vicsek model by using the topological structure of a dynamic network and combining the concept of the moderate degree of complexity network. This method can improve the convergence speed and consistency of the system. Aiming at the problem that convergence efficiency of the Vicsek model is not high, Chen et al. [11] proposed a new rule that takes the median value of the movement direction of two neighboring individuals with the largest deviation of the movement direction within the set of individual neighborhoods as the motion direction of the next moment. The speed of the improved model under the control rule to achieve the direction uniformity is obviously accelerated. Jiang [12] proposed a heterogeneous speed adaptive cluster model based on the Vicsek model and studied the convergence speed and convergence probability of cluster. Tian [13] proposed a limited perspective model based on the Vicsek model and found that there is an optimal perspective

Manuscript received June 23, 2020.
*Corresponding author.
This work was supported by the National Natural Science Foundation of China (51979193), the China Scholarship Council (201506290080), the China Postdoctoral Science Foundation (2019M653652), and the Natural Science Basic Research Plan in Shaanxi Province of China (2019JQ-607).

for clusters, so that clusters can achieve synchronization as quickly as possible. Wang [14] added limited horizon constraints and neighborhood weights to the Vicsek model and studied the connectivity of ad-hoc communication networks. Olfati-Saber discussed how to use dynamic networks to model the behavior of multi-agent clusters [15], and extended the idea of multi-agents clustering in free space to multi-obstacle space [16]. The Olfati-Saber algorithm uses an improved potential field function to enable agents to avoid obstacles and move toward the target point, which improves the limitation of potential field traps and has become a classic multi-agents cluster control algorithm. Ye et al. [17] studied the aggregation and segmentation evolutionary behavior of the cluster system. Luo et al. [18] studied the cluster behavior of the pigeon herd. Li et al. [19] established a dynamic model of the cluster with an attention mechanism.

To solve the problem of low convergence efficiency of the Vicsek model, this paper proposes to add static summoning points based on the classic Vicsek model, so that the movements of all individuals in the group can quickly reach a consensus according to the summoning direction, and the equation of movement direction update in the Vicsek model is improved. The cluster consistency verification experiment is designed for verifying the effectiveness of the Vicsek with static summoning points (VSSP) algorithm in this paper. To verify the superiority of the VSSP algorithm, the Vicsek algorithm and the Olfati Saber algorithm are compared with the VSSP algorithm respectively, and the algorithm performance comparison verification experiment is designed. The experimental results verify the good performance of the algorithm in this paper. This algorithm can provide a reference for efficient cluster segmentation movement.

2. Classic Vicsek model

The Vicsek model [20−30] is a discrete-time cluster system composed of N autonomous individuals. They move at the same speed v in the plane, and the course angle of each individual is updated according to the average of its neighbors' course angles vector. The neighbors of individual i consist of individuals centered on the individual's current position $(x_i(t), y_i(t))$ and having a Euclidean distance from the individual less than the normal number r. $N_i(t)$ is used to express the neighbors of individual i at time t, that is

$$N_i(t) = \{j / d_{ij}(t) < r\}, \tag{1}$$

$$d_{ij} = \sqrt{(x_i(t) - x_j(t))^2 + (y_i(t) - y_j(t))^2}. \tag{2}$$

Each individual is its own neighbor. Each moves at a constant positive speed v in the plane, so the position of each individual is updated as

$$\begin{cases} x_i(t+1) = x_i(t) + v\cos\theta_i(t) \\ y_i(t+1) = y_i(t) + v\sin\theta_i(t) \end{cases}, \quad i = 1, 2, \cdots, N \tag{3}$$

where $\theta_i(t)$ is the course angle of individual i at time t, which is updated as

$$\theta_i(t+1) = \arctan \frac{\sum\limits_{j \in N_i(t)} \sin\theta_j(t)}{\sum\limits_{j \in N_i(t)} \cos\theta_j(t)}. \tag{4}$$

It is noted that the dynamic behavior of the above system is completely determined by the initial state (initial course angle and initial position), the neighborhood radius r, and the movement speed v. The neighbors of each individual are determined by the position of other individuals, and the course angle of each individual is determined by the neighbors' course angle. Similarly, the course angle also affects the position. Therefore, a complex non-linear relationship is formed between the positions and course angles of all individuals.

Synchronization of the multi-agent system above means that the course angles of all individuals meet the condition:

$$\lim_{t \to \infty} \theta_i(t) = \theta, \quad i = 1, 2, \cdots, N \tag{5}$$

where θ may depend on the initial state $\{\theta_i(0), x_i(0), y_i(0), i = 1, 2, \cdots, N\}$ and the system parameters v, r.

3. An improved Vicsek model with static summoning points

Because of the low convergence efficiency of the Vicsek model which describes the dynamic behavior of cluster, this paper proposes to add static summoning points based on the classic Vicsek model for making all the individual movements in the group quickly reach a consensus according to the summoning direction, and the movement direction update equation of the Vicsek model and its linearized model is replaced.

3.1 Individual classification of the initial group

All individuals in the cluster will be guided by summoning points in the process of movement. When there are multiple summoning points, it is necessary to classify all the individuals in the group first, and clarify the subcluster guided by each summoning point, because dynamic behavior of the cluster system based on the Vicsek model is completely determined by the initial state (initial course angle and initial position), the neighborhood radius r, and the movement speed v. When the neighborhood radius and movement speed of the cluster system are given, movement of the cluster system is completely

determined by the initial course angle and position of each individual. Therefore, the classification of subclusters is also based on the course angle and position of the cluster at the initial state.

Suppose there are P static summoning points in the system, and the position of summoning point p is expressed as (x_p, y_p) (p=1,2, ⋯, P). $\boldsymbol{R_p}$ is used to represent the subcluster guided by the summoning point p in the cluster. To make the cluster reach the consensus quickly at the summoning direction in the optimal state, the total movement cost of the individual to each summoning point (distance cost and summoning diversion cost) needs to be considered to ensure that each individual is assigned to the summoning point with the minimal total movement cost.

3.1.1 Total cost model of movement

(i) Distance cost

The distance cost of individual i in the subcluster guided by summoning point p at time t is recorded as $dc_{ip}(t)$. The distance cost is the normalized value of Euclidean distance from the individual to the summoning point.

$$dc_{ip}(t) = \frac{d_{ip}(t) - \min(d_{iq}(t))}{\max(d_{iq}(t)) - \min(d_{iq}(t))}, \quad q = 1,2,\cdots,P \tag{6}$$

(ii) Summoning diversion angle cost

As shown in Fig.1, the course angle of individual i at time t is denoted as $\theta_i(t)$. The angle between the direct line of individual i at time t pointing to summoning point p and the horizontal coordinate axis is defined as the summoning angle of the summoning point to the individual, which is denoted as $\gamma_{ip}(t)$. The summoning diversion angle $\psi_{ip}(t)$ of summoning point p to the individual i at time t is the difference between the course angle of individual i and the summoning angle of summoning point p to the individual i. The summoning diversion angle cost of summoning point p to the individual i is recorded as $\psi c_{ip}(t)$, and the summoning diversion angle cost is the normalized value of the summoning diversion angle from the summoning point to the individual.

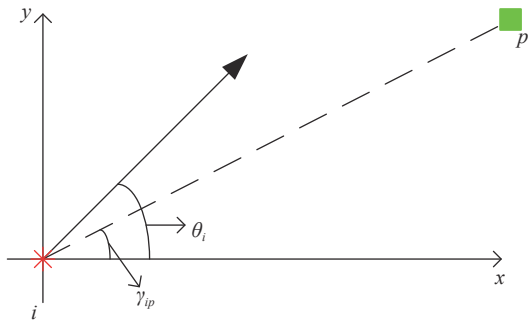

Fig. 1 Summoning diversion angle diagram

$$\gamma_{ip}(t) = \arctan\left[\frac{y_p(t) - y_i(t)}{x_p(t) - x_i(t)}\right] \tag{7}$$

$$\psi_{ip}(t) = \theta_i(t) - \gamma_{ip}(t) \tag{8}$$

$$\psi c_{ip}(t) = \frac{\psi_{ip}(t) - \min(\psi_{iq}(t))}{\max(\psi_{iq}(t)) - \min(\psi_{iq}(t))}, \quad q = 1,2,\cdots,P \tag{9}$$

(iii) Movement total cost

The movement total cost $Mc_{ip}(t)$ is the weighted sum of distance cost and summoning diversion angle cost when individual i is classified into subclusters of summoning point p at time t. Distance cost coefficient d_{coef} and summoning diversion angle cost coefficient ψ_{coef} are introduced respectively, and they meet the requirement of $d_{coef} + \psi_{coef} = 1$.

$$Mc_{ip}(t) = d_{coef} \cdot dc_{ip}(t) + \psi_{coef} \cdot \psi c_{ip}(t) \tag{10}$$

3.1.2 Individual classification rules in the initial cluster

The individual classification in the cluster is completely determined by the course angle and position of the group in an initial state, and the total movement cost matrix of the cluster at the initial time is denoted as $\boldsymbol{Mc_{N\times P}}$.

Definition 1 Suppose $\boldsymbol{A}$ is a matrix, and min ($\boldsymbol{A}$, 1) returns the column position where the minimum value of each row in matrix $\boldsymbol{A}$ is located. The vector $\boldsymbol{Rc}$ is the summoning point typeset with the lowest total cost of all individuals in the cluster.

$$\boldsymbol{Rc} = \min(\boldsymbol{Mc_{N\times P}}, 1) = \min\left(\begin{bmatrix} Mc_{11} & \cdots & Mc_{1q} & \cdots & Mc_{1P} \\ \vdots & \vdots & \vdots & \vdots & \vdots \\ Mc_{i1} & \cdots & Mc_{iq} & \cdots & Mc_{iP} \\ \vdots & \vdots & \vdots & \vdots & \vdots \\ Mc_{N1} & \cdots & Mc_{Nq} & \cdots & Mc_{NP} \end{bmatrix}, 1\right) = \begin{bmatrix} Rc_1 \\ \vdots \\ Rc_i \\ \vdots \\ Rc_N \end{bmatrix} \tag{11}$$

Then the subcluster $\boldsymbol{R_p}$ guided by summoning point p can be expressed as

$$\boldsymbol{R_p} = \{i / Rc_i = p\}. \tag{12}$$

Thus, the types of summoning points to which all the individuals in the cluster belong have been determined, and all individuals in the subcluster $\boldsymbol{R_p}$ will quickly reach a consensus in the optimal state according to the direction of summoning point p.

3.2 Updating equation of course angle

In this paper, static summoning points are added to increase course guidance factors in the movement process of individuals in the cluster. The updating formula of the course angle in the typical Vicsek model needs to be modified under the considering of influence from static summoning points. The updated formula of the modified course angle is

$$\theta_i(t+1)=\arctan\frac{\sum_{j\in N_i(t)}\sin\theta_j(t)}{\sum_{j\in N_i(t)}\cos\theta_j(t)}+\eta\cdot\psi_{ip}(t) \tag{13}$$

where η is the summoning factor, $\eta\in(0,1)$.

4. Simulation and analysis

The improved Vicsek algorithm with static summoning points has a good cluster segmentation effect, and the convergence speed has been greatly improved. To verify the effectiveness of the algorithm proposed in this paper, a cluster segmentation consistency verification experiment is carried out. Because the summoning factor has a great influence on the convergence speed of the cluster movement, this paper has carried out comparative simulation experiments under different summoning factors. To verify the superiority of the algorithm proposed in this paper, the performance comparison experiment is designed.

Parameter settings: N=300, P=3, r=0.8, v=0.02, d_{coef}=0.4, ψ_{coef}=0.6, coordinates of the summoning points set {(0,0), (3,6), (6,0)}, η is set by 0.3, 0.25, 0.15 respectively. At the initial time, the cluster is randomly distributed in the square range of ([2,4], [2,4]) with the Gaussian distribution. The simulation step is unit 1 and the number of iterations is 120.

To quantitatively evaluate the convergence consistency and convergence speed of the designed algorithm, the quantitative evaluation index of maneuver consistency parameter and convergence time defined in [31] are cited. The maneuver consistency parameter V_P and convergence time T_c are expressed as

$$V_P(t)=\frac{1}{Nv_0}\cdot\sum_{p=1}^{P}\left\|\sum_{i\in\boldsymbol{R}_p}\boldsymbol{v}_i(t)\right\|, \tag{14}$$

$$T_c=\min_{V_P(t)\geqslant 0.99} t. \tag{15}$$

4.1 Verification of cluster segmentation consistency

In this paper, three groups of simulation experiments are carried out when the summoning factor values are 0.3, 0.25 and 0.15 respectively. Fig. 2 shows the spatial distribution state of cluster individuals at typical times when η=0.15 (the spatial dynamic distribution state of cluster individuals at η =0.3 and η =0.25 is similar to that at η=0.15, which will not be shown here). The arrow direction of each point in Fig. 2 is the direction of the individual at this moment, and the black solid box is the summoning point, the points marked in red, blue, and green are used to represent the subclusters classified into summoning points (0,0), (3,6), (6,0) respectively.

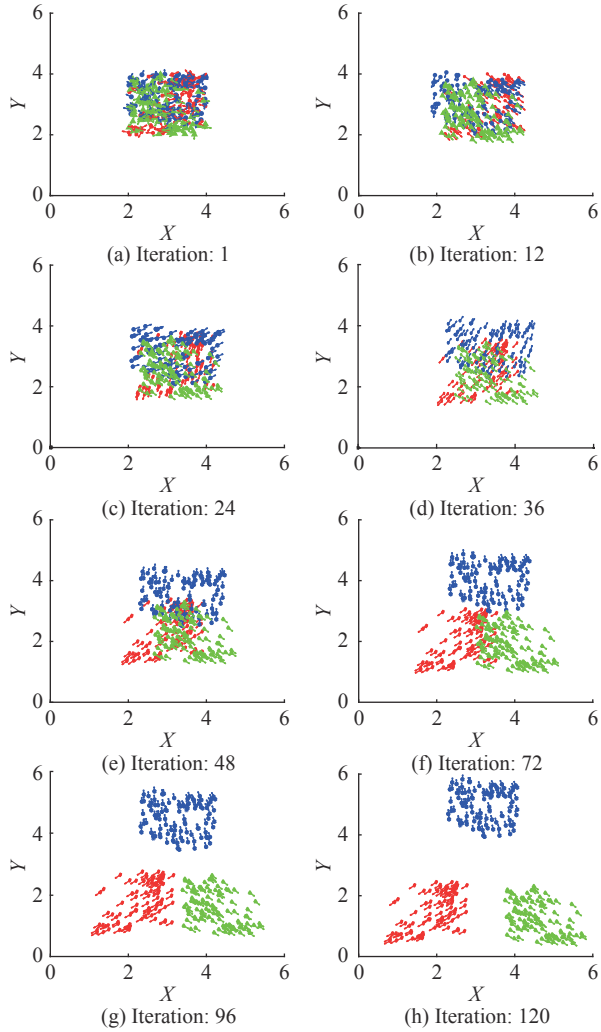

Fig. 2 Spatial distribution of individuals in a cluster at the typical time when η= 0.15

It can be seen from Fig. 2 that under the guidance of the summoning point, each subcluster quickly separates and moves to the corresponding summoning point. At the beginning of the cluster movement, each individual is constantly adjusting his course due to the great initial course difference of each individual. It makes subcluster course of the same summoning point reach the same, so there will be the phenomenon of individual wandering near the initial position. When all individuals adjust their

course angles to reach the same direction as the summoning point, the subclusters will be quickly separated. It can be seen that the subclusters are completely separated and the cluster segmentation consistency is good.

4.2 Effect of summoning factor on the convergence rate

To analyze the influence of the summoning factor on the convergence rate of the cluster, three groups of simulation comparison experiments are carried out when the summoning factor values are 0.3, 0.25 and 0.15 respectively, the results are shown in Fig. 3 to Fig. 5.

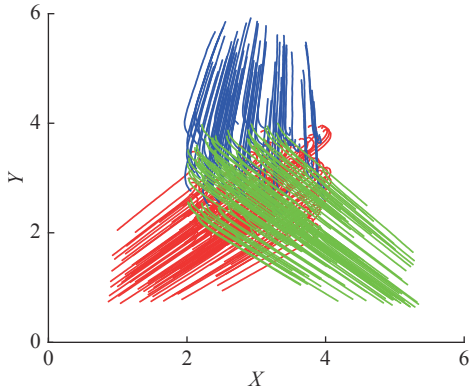

(a) Trajectories of all individuals in the cluster

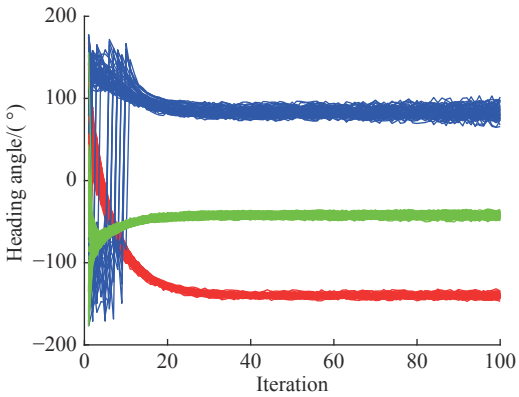

(b) Course angle-time curve of all individuals in the cluster

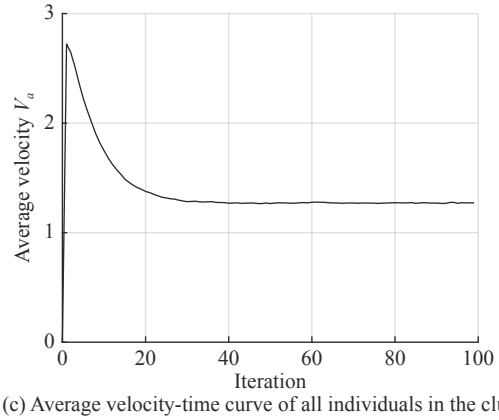

(c) Average velocity-time curve of all individuals in the cluster

Fig. 3 Simulation results when η=0.3

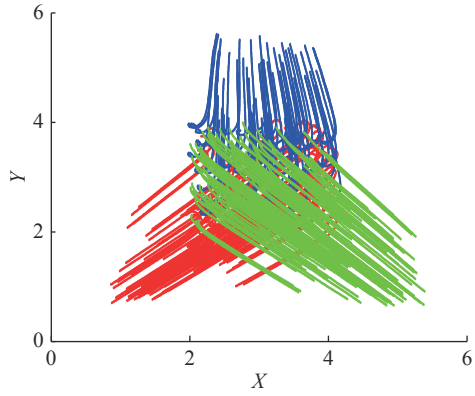

(a) Trajectories of all individuals in the cluster

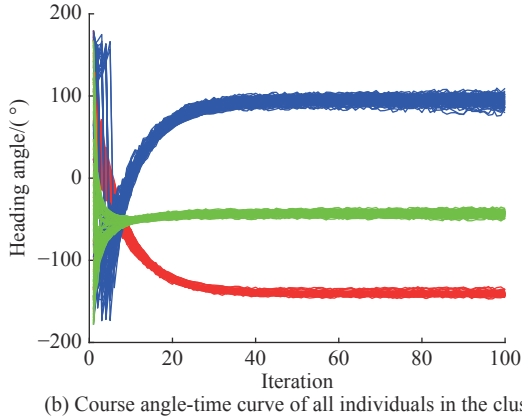

(b) Course angle-time curve of all individuals in the cluster

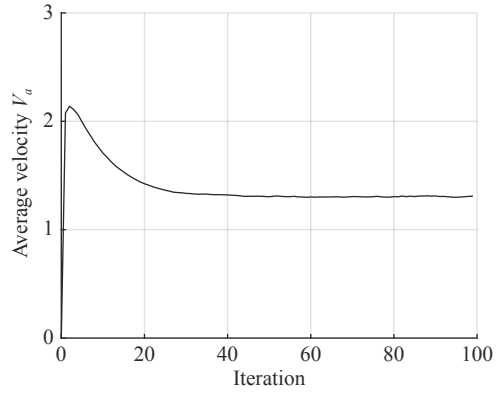

(c) Average velocity-time curve of all individuals in the cluster

Fig. 4 Simulation results when η=0.25

According to the simulation results: (i) With the decrease of the summoning factor, the convergence rate of a cluster is slowing down. When η=0.3, the course angles of all individuals in the cluster tend to be consistent after about 25 iterations, when η=0.25, that tends to be consistent after about 32 iterations, when η=0.15, it tends to be consistent after about 50 iterations. (ii) The trajectory of individuals in the cluster changes greatly in the early stage of the movement. This is because before course angles of subclusters reaching consistent, the course angles of subclusters are constantly adjusted under the

guidance of the summoning point. (iii) The final course angles of the subclusters guided by the three summoning points converge to −135°, 90° and −45° respectively, and the cluster segmentation has a good consistency. (iv) At the beginning of the calculation, the course angle-time curve of individuals show the oscillation of the course angle. This is because the updating of the course angle is related to the course angle of other individuals in its neighborhood, where individuals belong to a subcluster of another summoning point, which has an impact on the update of the course angle.

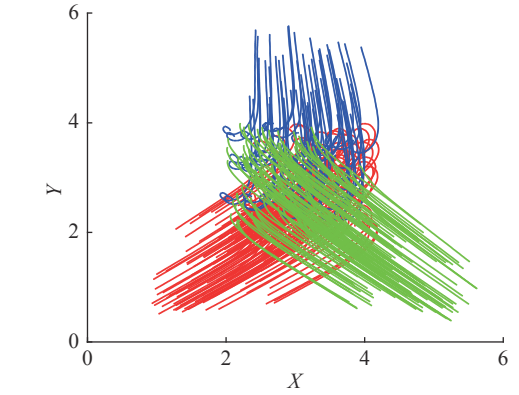

(a) Trajectories of all individuals in the cluster

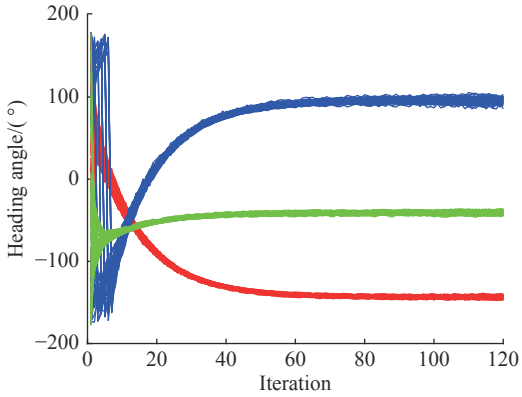

(b) Course angle-time curve of all individuals in the cluster

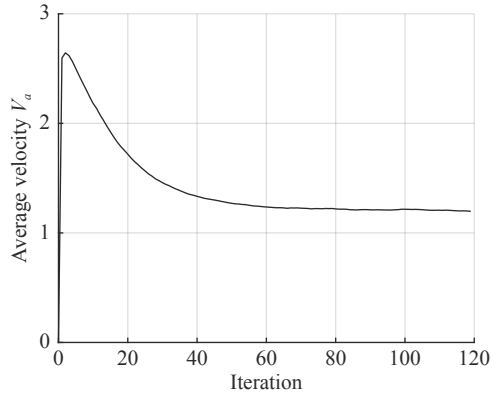

(c) Average velocity-time curve of all individuals in the cluster

Fig. 5 Simulation results when η=0.15

4.3 Comparison and verification of algorithm performance

4.3.1 Comparison and verification for cluster segmentation consistency of different algorithms

To verify the superiority of the VSSP algorithm proposed in this paper, the performance of the basic Vicsek algorithm and the classic Olfati-Saber algorithm in this field are compared with the VSSP algorithm. In the simulation environment of Section 4.1, simulation experiments are carried out based on the VSSP algorithm, the Olfati-Saber algorithm, and the basic Vicsek algorithm. The summoning factor in the environment is $\eta = 0.45$. Fig. 6 shows the comparison results of the maneuver consistency parameter time history curves of the three algorithms. Table 1 shows the comparison results of the convergence time indicator of the three algorithms in the environment.

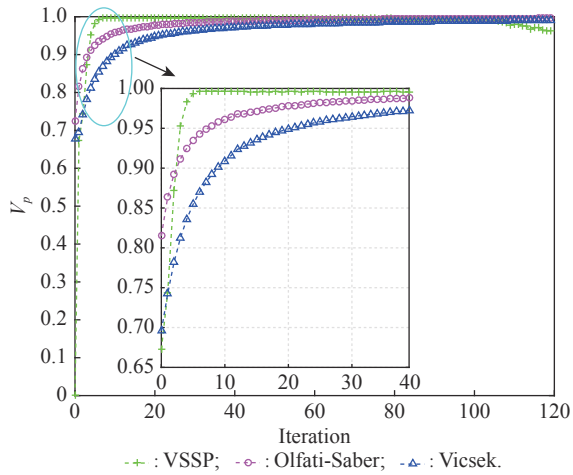

Fig. 6 Time history curve of maneuver consistency parameter V_P for the three algorithms when η=0.45

Table 1 Comparison results of the convergence time indicator T_c of the three algorithms when η=0.45

Parameter	VSSP	Olfati-Saber	Vicsek
T_c	6	35	62

From the simulation results in Fig. 6 and Table 1, the following conclusions can be drawn: (i) Whether it is comparing the maneuver consistency parameter V_P or comparing the convergence time indicator T_c, not only the convergence consistency of the VSSP algorithm proposed in this paper is superior to the Olfati-Saber algorithm and the basic Vicsek algorithm, but also the convergence time is significantly shorter than the other two

algorithms. (ii) The Olfati-Saber algorithm converges very quickly in the initial stage, but within a relatively high convergence consistency range, its convergence rate is slow. However, the VSSP algorithm converges at a faster convergence rate throughout the entire process, which shows a better convergence performance. Through the comparative experiments, the superiority of the algorithm proposed in this paper can be verified. (iii) The comparison results between the VSSP algorithm and the basic Vicsek algorithm show that adding static summoning points to the typical Vicsek model can greatly improve the convergence performance of the cluster movement. The comparison results between the VSSP algorithm and the Olfati-Saber algorithm show that the algorithm proposed in this paper has certain advantages.

In order to further verify the superiority of the VSSP algorithm, different simulation environments need to be set up for horizontal comparison. In Subection 4.3.2, the three algorithms are compared and verified by setting up the simulation environments for clusters of different scales. And in Subection 4.3.3, the three algorithms are compared and verified by setting the simulation environment with different numbers of summoning points.

4.3.2 Comparison and verification of algorithms under different cluster scales

In this group of comparative experiments, the parameter settings are as follows: η=0.35，P=3，r=0.8，v=0.02，d_{coef}=0.4，ψ_{coef}=0.6. The summoning point set coordinate is {(0,0),(3,6),(6,0)}. The numbers of individuals are N_1=100, N_2=400, N_3=700. At the initial time, the cluster is randomly distributed in the square range of ([2,4], [2,4]) with the Gaussian distribution. The simulation step is unit 1 and the number of iterations is 90. Fig. 7 to Fig. 9 are the simulation results when the numbers of individuals in the cluster are 100, 400 and 700 respectively. Since the movement trajectories of all individuals in the cluster and the course angle-time curves of all individuals in the cluster obtained based on the three different algorithms are similar, the subgraphs (*a*) and (*b*) in Figs. 7−9 only show the simulation results based on the VSSP algorithm. Table 2 shows the comparison results of the convergence speed of different algorithms in the three environments.

From the simulation results in Figs. 7−9 and Table 2, the following conclusions can be drawn: (i) As the number of individuals in the cluster increases, the convergence speed of the maneuver consistency parameter V_P of the Olfati-Saber algorithm and the Vicsek algorithm becomes slower, and the convergence time index T_c becomes larger, while the convergence speed of the VSSP algorithm is almost unchanged. This shows that the VSSP algorithm has a strong adaptability to large-scale segmenting movement. (ii) When the cluster scale is small, the convergence speed of the Olfati-Saber algorithm is significantly better than that of the Vecsek algorithm, but as the cluster scale increases, the advantage of the Olfati-Saber algorithm gradually disappears.

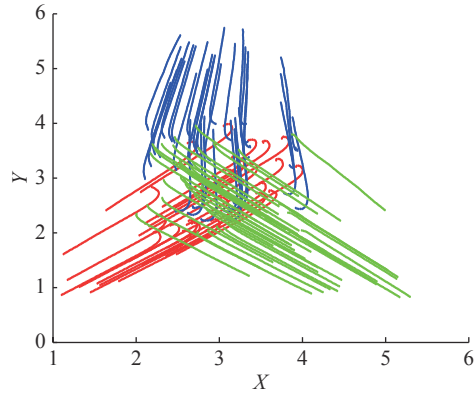

(a) Movement trajectory of individuals in the cluster based on the VSSP algorithm

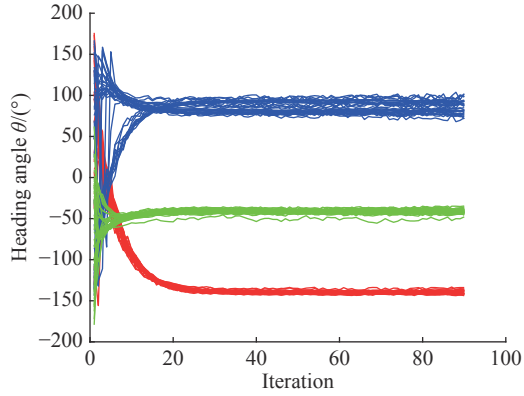

(b) Course angle-time curves of all individuals in the cluster based on the VSSP algorithm

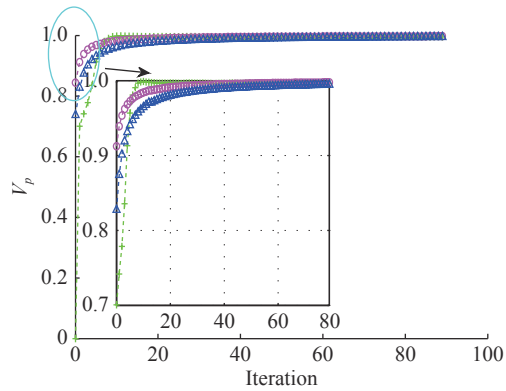

(c) Maneuver consistency parameter V_p-time curves of the three algorithms

-+- : VSSP; -o- : Olfati-Saber; -Δ-: Vicsek.

Fig. 7 Simulation results when N=100

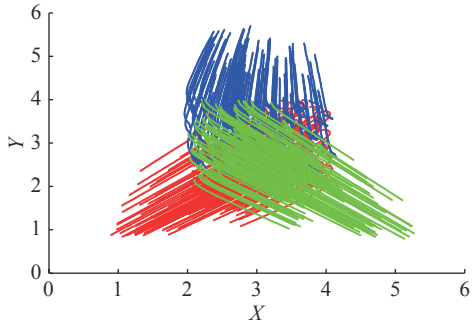

(a) Movement trajectory of individuals in the cluster based on the VSSP algorithm

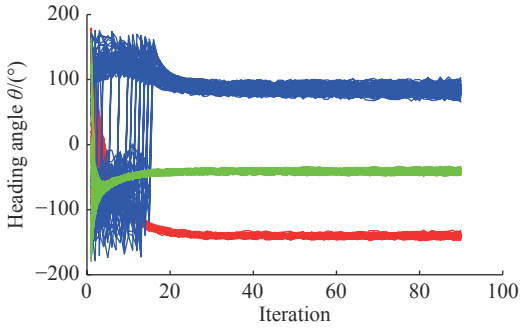

(b) Course angle-time curves of all individuals in the cluster based on the VSSP algorithm

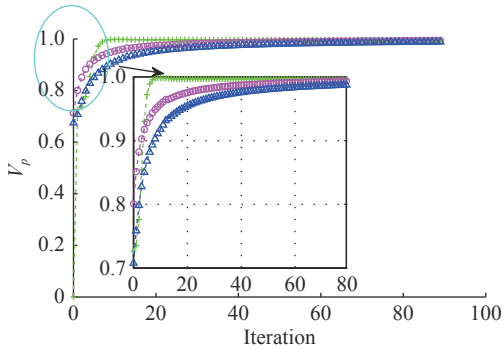

(c) Maneuver consistency parameter V_p-time curves of the three algorithms

-+-: VSSP; -o-: Olfati−Saber; -Δ-: Vicsek.

Fig. 8 Simulation results when N=400

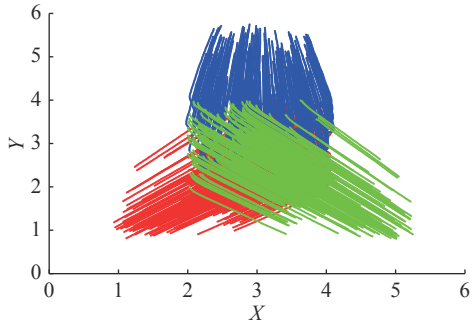

(a) Movement trajectory of individuals in the cluster based on the VSSP algorithm

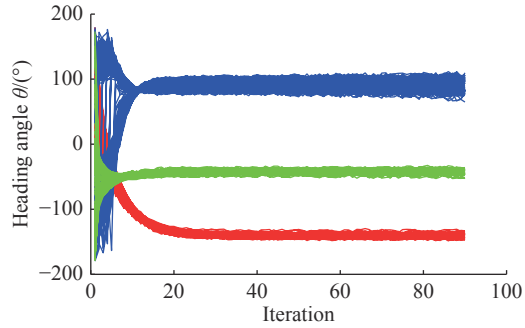

(b) Course angle-time curves of all individuals in the cluster based on the VSSP algorithm

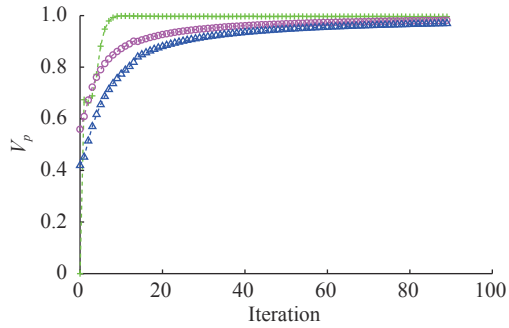

(c) Maneuver consistency parameter V_p-time curves of the three algorithms

-+-: VSSP; -o-: Olfati-Saber; -Δ-: Vicsek.

Fig. 9 Simulation results when N=700

Table 2 Comparison results of convergence time of different algorithms in the three environments

Parameter	Number of individuals	VSSP	Olfati-Saber	Vicsek
T_c	N=100	8	25	62
	N=400	6	48	70
	N=700	9	65	83

4.3.3 Comparison and verification of algorithms under different summoning points

In this group of comparative experiments, the parameter settings are as follows: N=300，η=0.45，P=3，r=0.8，v=0.02，d_{coef}=0.4，ψ_{coef}=0.6. When the number of summoning points P_1=2, the coordinate of the summoning point set is {(0,0), (6,6)}; when P_2=4, the coordinate of the summoning point set is {(0,0), (0,6), (6,0), (6,6)}; when P_3=6, the coordinate of the summoning point set is {(3,0), (0,1.5), (0,4.5), (3,6), (6,4.5), (6,1.5)}; when P_4=8, the coordinate of the summoning point set is {(1.5,0), (0,1.5), (0,4.5), (1.5,6), (4.5,6), (6,4.5), (6,1.5), (4.5,0)}. At the initial time, the cluster is randomly distributed in the square range of ([2,4], [2,4]) with the Gaussian distribution. The simulation step is unit 1 and the number of it-

erations is 90 times. Figs. 10−13 are the simulation results when the numbers of summoning points in the cluster are 2, 4, 6 and 8 respectively. Since the movement trajectories of all individuals in the cluster and the course angle-time curves of all individuals in the cluster obtained based on the three different algorithms are similar, the subgraphs (c) and (d) in Figs. 10−13 only show the simulation results based on the VSSP algorithm. Table 3 shows the comparison results of the convergence speed of different algorithms in the four environments.

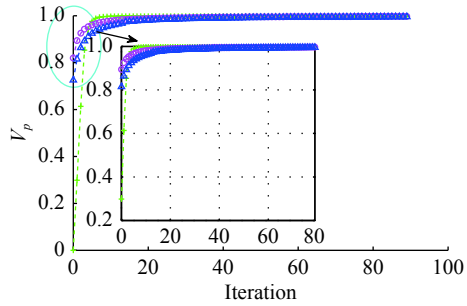

(e) Maneuver consistency parameter V_p-time curves of the three algorithms

-+-: VSSP; -o-: Olfati-Saber; -△-: Vicsek.

Fig. 10 Simulation results when the number of summoning points *P*=2

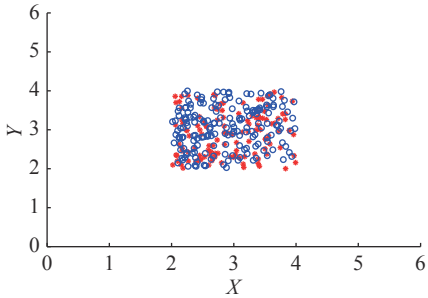

(a) Initial state of cluster

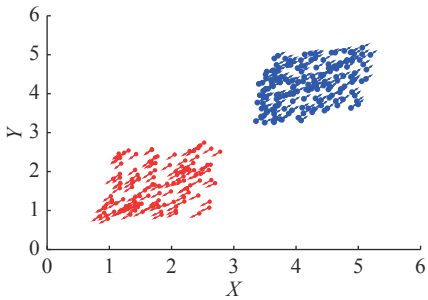

(b) State of cluster when the number of iterations is 90

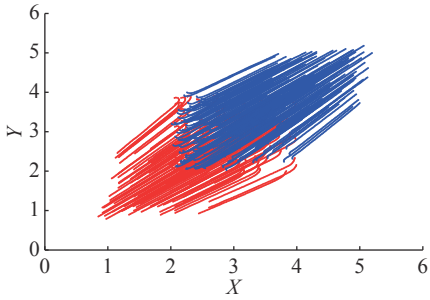

(c) Movement trajectory of individuals in the cluster based on the VSSP algorithm

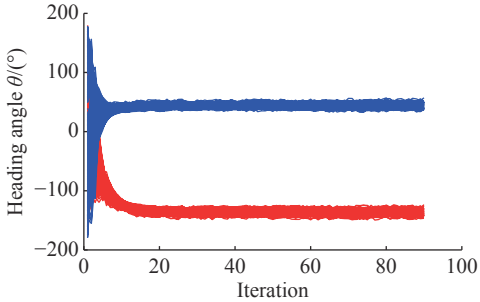

(d) Course angle-time curves of all individuals in the cluster based on the VSSP algorithm

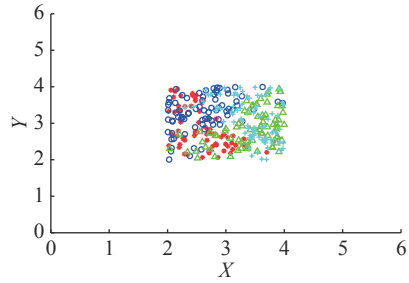

(a) Initial state of cluster

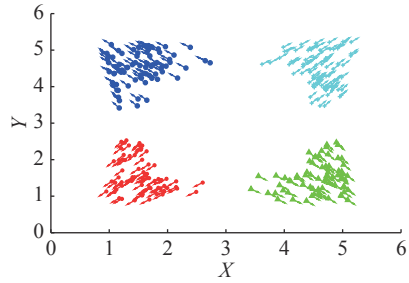

(b) State of cluster when the number of iterations is 90

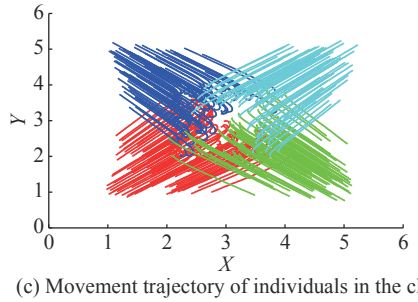

(c) Movement trajectory of individuals in the cluster based on the VSSP algorithm

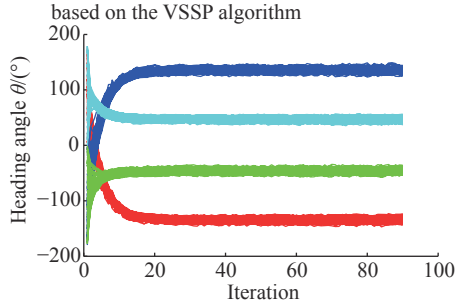

(d) Course angle-time curves of all individuals in the cluster based on the VSSP algorithm

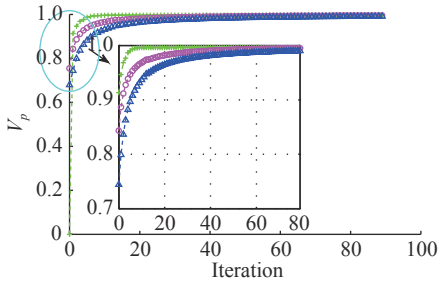

(e) Maneuver consistency parameter V_P-time curves of the three algorithms

-+-: VSSP; -○-: Olfati-Saber; -△-: Vicsek.

Fig. 11 Simulation results when the number of summoning points *P*=4

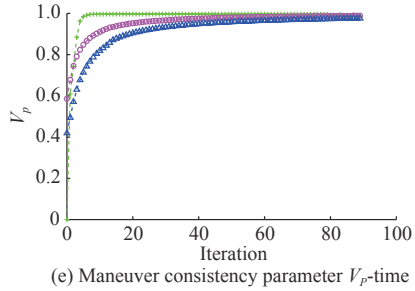

(e) Maneuver consistency parameter V_P-time curves of the three algorithms

-+-: VSSP; -○-: Olfati-Saber; -△-: Vicsek.

Fig. 12 Simulation results when the number of summoning points *P*=6

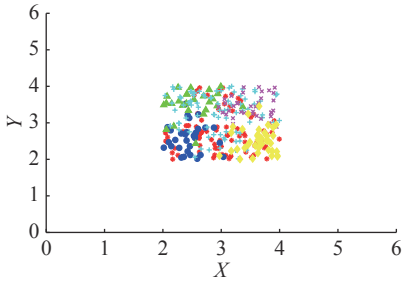

(a) Initial state of cluster

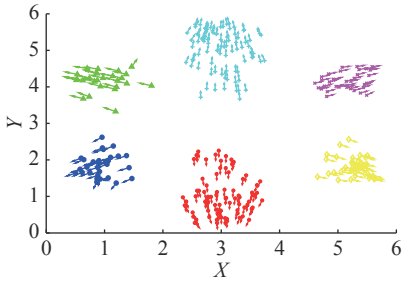

(b) State of cluster when the number of iterations is 90

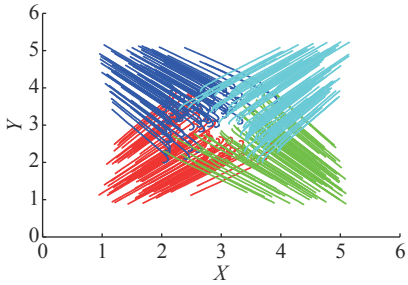

(c) Movement trajectory of individuals in the cluster based on the VSSP algorithm

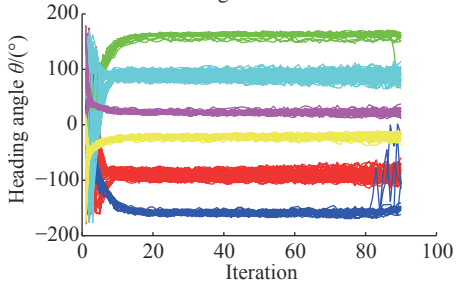

(d) Course angle-time curves of all individuals in the cluster based on the VSSP algorithm

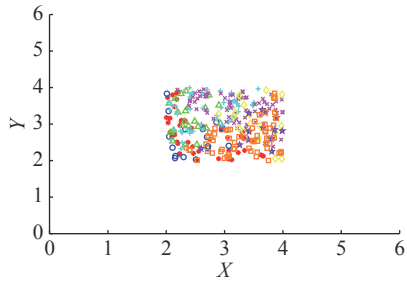

(a) Initial state of cluster

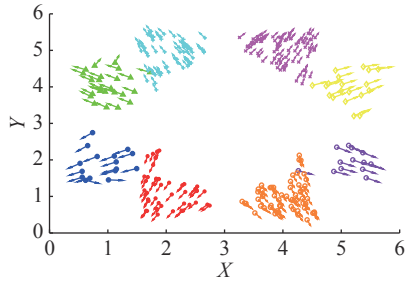

(b) State of cluster when the number of iterations is 90

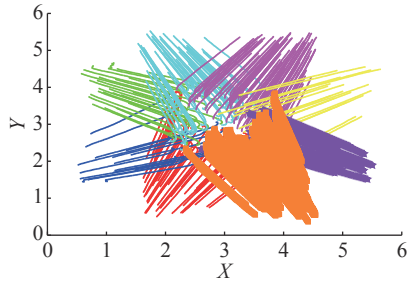

(c) Movement trajectory of individuals in the cluster based on the VSSP algorithm

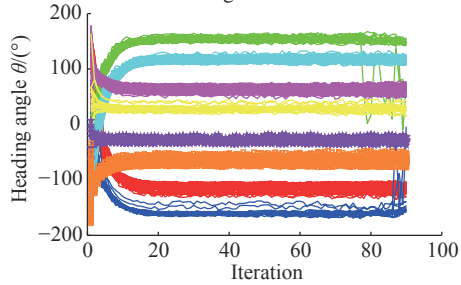

(d) Course angle-time curves of all individuals in the cluster based on the VSSP algorithm

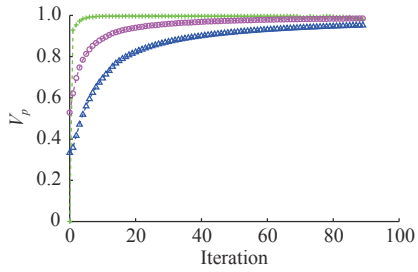

(e) Maneuver consistency parameter V_p-time curves of the three algorithms

-+-: VSSP; -o-: Olfati-Saber; -△-: Vicsek.

Fig. 13 Simulation results when the number of summoning points *P*=8

Table 3 Comparison results of convergence time of different algorithms in the four environments

Parameter	Number of summoning points	VSSP	Olfati-Saber	Vicsek
T_c	*P*=2	5	12	18
	P=4	6	21	29
	P=6	9	53	64
	P=8	12	65	89

From the simulation results in Figs. 10−13 and Table 3, the following conclusions can be drawn: (i) As the number of summoning points in the environment increases, the more types of clusters need to be classified, the more difficult it is to segment the clusters, and the convergence speed of the three algorithms is all slowed down. (ii) With the increase of cluster classification, the segmentation performance of the Olfati-Saber algorithm and the Vicsek algorithm deteriorates sharply, while the VSSP algorithm shows a strong adaptability.

5. Conclusions

In this paper, based on the typical Vicsek model, static summoning points are introduced to guide the individuals in the cluster to be classified into subclusters, and each subcluster gathers to its corresponding summoning points. It can be seen from the simulation experiment that adding static summoning points to the Vicsek model can greatly improve the convergence rate of the cluster movement, and at the same time make the cluster maintain good course consistency. Through the comparative experiments of different summoning factors, we can see that the summoning factor has a great influence on the convergence rate of the cluster, the larger the summoning factor is, the faster the convergence rate of the cluster is. Through comparison and verification with the typical algorithms of the Olfati-Saber algorithm and the basic Vicsek algorithm, we can see the superiority of the VSSP algorithm.

The method proposed in this paper can be well used in cluster segmentation, but in practice, the summoning points are more dynamic. Besides, the proposed method cannot be used for cluster gathering. These problems are what we need to further study later.

References

[1] LIANG X L, HE L L, ZHANG J Q. Configuration control and evolutionary mechanism of aircraft swarm. Scientia Sinica Technologica, 2019, 49(3): 277–287. (in Chinese)

[2] LIN D F, HE S M, WANG J, et al. On virtual leader-follower based distributed cooperative swarm guidance strategy. Scientia Sinica Technologica, 2016, 46(1): 79–88. (in Chinese)

[3] TIAN L, WANG M Y, ZHAN Q L, et al. Distributed time-varying group formation tracking for cluster systems under switching topologies. Scientia Sinica Informationis, 2020, 50(3): 408–423. (in Chinese)

[4] ZHOU W Q, ZHU J H, KUANG M C. An unmanned air combat system based on swarm intelligence. Scientia Sinica Informationis, 2020, 50(3): 363–374. (in Chinese)

[5] SELMA B, CHOURAQUI S, ABOUSISSA H. Fuzzy swarm trajectory tracking control of unmanned aerial vehicle. Journal of Computational Design and Engineering, 2020, 7(4): 435–447.

[6] BEJAOUI A, PART K H, ALOUINI M S. A QoS-oriented trajectory optimization in swarming unmanned-aerial-vehicles communications. IEEE Wireless Communications Letters, 2020, 9(6): 791–794.

[7] KELNER J M, ZIOLKOWSKI C. Effectiveness of mobile emitter location by cooperative swarm of unmanned aerial vehicles in various environmental conditions. Sensors, 2020, 20(9): 1–21.

[8] RAUL F R, ESSAM D, JUSTIN F. Electroencephalographic workload indicators during teleoperation of an unmanned aerial vehicle shepherding a swarm of unmanned ground vehicles in contested environments. Frontiers in Neuroscience, 2020. DOI:10.3389/fnins.2020.00040.

[9] HASSAN H, SEYED H S, JALAL K. Hybrid form of particle swarm optimization and genetic algorithm for optimal path planning in coverage mission by cooperated unmanned aerial vehicles. Journal of Aerospace Technology and Management, 2020, 12: 1–13.

[10] GAO J X, CHEN Z, CAI Y Z, et al. Approach to enhance convergence efficiency of Vicsek model. Control and Decision, 2009, 24(8): 1269–1272. (in Chinese)

[11] CHEN S M, SHU J, NIE S, et al. Convergence efficiency of a class of improved Vicsek model. Information and Control, 2011, 40(3): 318–322. (in Chinese)

[12] JIANG Y Y. Heterogeneous adaptive speed clustering system and emergent behavior based on Vicsek model. Guangxi Physics, 2013, 34(2): 22–25. (in Chinese)

[13] TIAN B M. Research of Vicsek model with a system of self-driven agents. Hefei: University of Science and Technology of China, 2009. (in Chinese)

[14] WANG X G. A modified Vicsek model for moving swarms with exponential neighbor weight and restricted visual field. Nanjing: Nanjing University of Aeronautics and Astronautics, 2013. (in Chinese)

[15] SABER R O. Flocking for multi-agent dynamic systems: algorithms and theory. IEEE Trans. on Automatic Control, 2006, 51(3): 401–420.

[16] SABER R O, FAX J A, MURRAY R M. Consensus and cooperation in networked multi-agent systems. Proceedings of

the IEEE, 2007, 95(1): 215–233.
[17] YE M. Analysis of aggregation and decentralized evolution behavior of collective dynamic systems. Wuhan: Huazhong University of Science & Technology, 2019. (in Chinese)
[18] LUO Q N, DUAN H B, FAN Y M. Analysis on stability and aggregation behavior of pigeon collective model. Scientia Sinica Technologica, 2019, 49(6): 652–660. (in Chinese)
[19] LI P, DUAN H B. A flocking model base on selective attention mechanism. Scientia Sinica Technologica, 2019, 49(9): 1040–1050. (in Chinese)
[20] VICSEK T, CZIROK A, BEN J E, et al. Novel type of phase transition in a system of self-driven particles. Physical Review Letters, 1995, 75(6): 1226–1229.
[21] LIU Z X, GUO L. Connection and synchronization of Vicsek model. Scientia Sinica Informationis, 2007, 37(8): 979–988. (in Chinese)
[22] ROY S, SHIRAZI M J, JANTZEN B. Effect of visual and auditory sensing cues on collective behavior in Vicsek models. Physical Review E, 2019, 100(6): 062415.
[23] MORENO J C, PUZZO M, PAUL W. Collective dynamics of pedestrians in a corridor: an approach combining social force and Vicsek models. Physical Review E, 2020, 102(2): 022307.
[24] CAMBUI D S. Vicsek model of self-propelled particles with hybrid noise. Modern Physics Letters B, 2020, 34(14): 2050144.
[25] KATYAL N, DEY S, DAS D, et al. Coarsening dynamics in the Vicsek model of active matter. European Physical Journal E, 2020. DOI: 10.1140/epje/i2020-11934-3.
[26] NARIZUKA T, YAMAZAKI Y. Lifetime distributions for adjacency relationships in a Vicsek model. Physical Review E, 2020, 100(3): 032603.
[27] RUBIO P, LETICIA M, VIRGILIIS D, et al. Self-propelled Vicsek particles at low speed and low density. Physical Review E, 2019, 99(5): 052602.
[28] BARBERIS L. Emergence of a single cluster in Vicsek 's model at very low noise. Physical Review E, 2018, 98(3): 032607.
[29] MARTINEZ R, ALARCON F, ROGEL R D, et al. Collective behavior of Vicsek particles without and with obstacles. European Physical Journal E, 2018. DOI: 10.1140/epje/i2018-11706-8.
[30] GULICH D, BAGLIETTO G, ROZENFELD A F. Temporal correlations in the Vicsek model with vectorial noise. Physica A-Statistical Mechanics and its Applications, 2018, 502: 590–604.
[31] DUAN H B, QIU H X. Unmanned aerial vehicle swarm autonomous control based on swarm intellignce. Beijing: Science Press, 2018. (in Chinese)

Biographies

MA Yan was born in 1991. He is currently a doctoral student at the Key Laboratory of Unmanned Underwater Vehicle, Ministry of Industry and Information Technology, School of Marine Science and Technology, Northwestern Polytechnical University. His research interests include clustering computation, unmanned systems, and intelligent control.
E-mail: AI_worshipper@163.com

MAO Zhaoyong was born in 1980. He is a professor in the School of Marine Science and Technology, Northwestern Polytechnical University, China. His research interests include unmanned underwater vehicles, reliability optimization, and ocean energy harvesting.
E-mail: maozhaoyong@nwpu.edu.cn

QIN Jian was born in 1978. He received his Ph.D. degree in engineering mechanics from Beijing Institute of Technology, Beijing, China, in 2013. He is a research fellow with the Naval Research Academy. His research interests include engineering mechanics and robot control.

MENG Xiangyao was born in 1987. He received his Ph.D. degree in mechanical engineering from Northwestern Polytechnical University, Xi'an, Shaanxi, China, in 2015. From 2015 to now, he is an assistant research fellow with the Naval Research Academy. His research interest is unmanned underwater system.
E-mail: xiangyao_meng@126.com

XIAO Yujie was born in 1987. He received his master's degree in electrical engineering in 2013 and Ph.D. degree in systems engineering in 2015. From 2015 to now, he is an associate research fellow with the Naval Research Academy. His research interests include unmanned formation cooperative control and intelligent decision system.
E-mail: 825807129@qq.com

CHEN Jianhua was born in 1989. He received his Ph.D. degree in mechanical engineering from Mechanical Engineering College, Shijiazhuang, Hebei, China, in 2018. From 2018 to now, he is an assistant research fellow with the Naval Research Academy. His research interests include unmanned surface vehicle and robot control.
E-mail: chenjhua@zju.edu.cn

FENG Wei was born in 1988. He received his Ph.D. degree from Naval University of Engineering, Wuhan, Hubei, China, in 2018. From 2018 to now, he is an assistant research fellow with the Naval Research Academy. His research interest is the unmanned underwater system.
E-mail: hjgcdxfw@163.com